Journal of Applied Polymer Science

Donor Copolymer with Benzo[1,2-b:4,5-b′]dithiophene and Quinoxaline Derivative Segments for Photovoltaic Applications

Zhi Gao,[1] Bo Qu,[1] Haimei Wu,[2] Chao Gao,[2] Hongsheng Yang,[1] Lipei Zhang,[1] Lixin Xiao,[1] Zhijian Chen,[1] Qihuang Gong[1]

[1]State Key Laboratory for Artificial Microstructures and Mesoscopic Physics, Department of Physics, Peking University, Beijing 100871, People's Republic of China

[2]Xi'an Modern Chemistry Research Institute, Xi'an, Shaanxi 710065, People's Republic of China

Correspondence to: B. Qu (E-mail: bqu@pku.edu.cn), C. Gao (E-mail: chaogao74@gmail.com), or Q. Gong (E-mail: qhgong@pku.edu.cn)

ABSTRACT: A donor copolymer Poly{2,6-4,8-bis(2-ethylhexyl)benzo[1,2-b:3,4-b′]dithiophene-5,8-2,3-bis(5-octylthiophen-2-yl)quinoxaline} (PBDTThQx) with benzo[1,2-b:4,5-b′]dithiophene and quinoxaline derivatives was synthesized and characterized with NMR, ultraviolet–visible spectroscopy, thermogravimetric analyses, and cyclic voltammetry. Photovoltaic devices with the configuration in dium tin oxide–poly(3,4-ethylenedioxythiophene)–poly(styrene sulfonate)–PBDTThQx–[6,6]-phenyl-C_{61}-butyric acid methyl ester ($PC_{61}BM$)–LiF–Al were fabricated, in which PBDTThQx performed as the electron donor and $PC_{61}BM$ was the electron acceptor in the active layer. The device presented reasonable photovoltaic properties when the weight ratio of PBDTThQx:$PC_{61}BM$ reached 1:3. The open-circuit voltage, fill factor, and power conversion efficiency were gauged to be 0.75 V, 0.59, and 0.74%, respectively. The experimental data implied that PBDTThQx would be a promising donor candidate in the application of polymer solar cells. © 2013 Wiley Periodicals, Inc. J. Appl. Polym. Sci. **2014**, *131*, 40279.

KEYWORDS: copolymers; films; functionalization of polymers; optical and photovoltaic applications

Received 25 July 2013; accepted 9 December 2013
DOI: 10.1002/app.40279

INTRODUCTION

Because of their light weight, low cost, large area, and flexibility, organic photovoltaic devices (OPVs) based on the bulk-heterojunction active layers of conjugated polymers and fullerene derivatives have drawn wide attention.[1–4] Generally speaking, poly(3-hexylthiophene) (P3HT) and methanofullerene (6,6)-phenyl-C_{61}-butyric acid methyl ester ($PC_{61}BM$) are commonly used donors and acceptors in the active layer, respectively.[5,6] However, the relatively large band gap of P3HT limits the absorption capability and spectrum response range of the active layer. Moreover, the high highest occupied molecular orbital (HOMO) level of P3HT induces a low open-circuit voltage (V_{oc}) in OPVs; this confines the power conversion efficiency (PCE) of the devices. Much effort has been made in the OPV field to pursue novel donor–acceptor (D–A) copolymers with low HOMO levels and narrow band gaps.[7–17] According to previous studies, benzo[1,2-b:4,5-b′]dithiophene (BDT)-based moieties, such as 4,7-dithiophene-2-yl-2,1,3-benzothiadiazole, thieno[3,4-b]thiophene, and *N*-alkylthieno-[3,4-c]-pyrrole-4,6-dione, have been considered to be effective donor segments in the main chain of polymers,[18–22] and promising photovoltaic properties have been realized accordingly. Meanwhile, because of the electron-deficient *N*-heterocycle, quinoxaline-based moieties, for example, poly[2,3-bis-(3-octyloxyphenyl)quinoxaline-5,8-diyl-alt-thiophene-2,5-diyl] (TQ1)[23] and Poly[N-9′-heptadecanyl-4,5-ethylenecarbazole-alt-5,8-bis(2′-thienyl)-2,3-bis(4-octyloxyphenyl)quinoxaline] (PECz-DTQx),[24] were introduced as acceptors into the main chain of the D–A copolymers. The energy levels of the copolymers could be effectively tuned. Therefore, the design of the D–A copolymers based on BDT and quinoxaline for photovoltaic devices would be a possible solution for the development of OPVs.

In a previous study, the copolymers Poly{2,6-4,8-bis(2-ethylhexyl)-benzo[1,2-b:3,4-b′]dithiophene-5,8-2,3-bis(3-(octyloxy)phenyl)quinoxaline} (PBDTQx) and Poly{2,6-4,8-bis(2-ethylhexyl)benzo[1,2-b:3,4-b′]dithiophene-5,8-6-fluorine-2,3-bis(3-(octyloxy)phenyl)quinoxaline} (PBDTFQx), which were based on BDT and quinoxaline, were synthesized and investigated in our laboratory.[4,25] Reasonable photovoltaic performances of the OPVs based on the copolymers were achieved. Moreover, to further improve the absorption capability of the photosensitive materials, an increase in the conjugation of the copolymers was considered to be an effective method. In

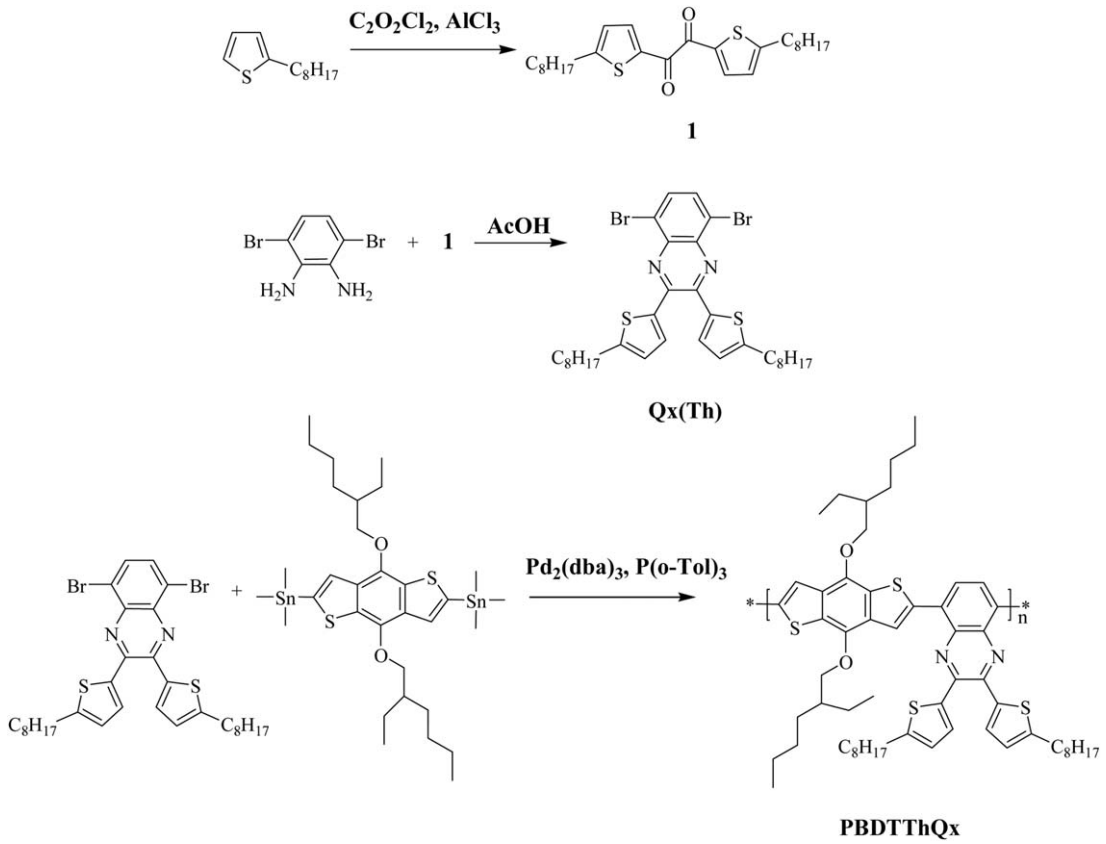

Scheme 1. Synthetic route to PBDTThQx.

this study, a donor copolymer Poly{2,6-4,8-bis(2-ethylhexyl)-benzo[1,2-b:3,4-b′]dithiophene-5,8-2,3-bis(5-octylthiophen-2-yl)quinoxaline} (PBDTThQx) was synthesized and is reported in this article (Scheme 1). The synthesis process, optical properties, and photovoltaic properties of the copolymer were investigated in detail. Quinoxaline derivative (ThQx) and BDT moieties performed as the acceptor and donor segments in the main chain of PBDTThQx, respectively. It is worth noting that the thiophene rings were introduced into the quinoxaline segments instead of the benzene rings; this indicated the prolonged conjugation length of the copolymer PBDTThQx. The photovoltaic properties of the PBDTThQx-based OPVs were acceptable in this study. With an optimized blend ratio of PBDTThQx to $PC_{61}BM$, the OPVs exhibited V_{oc}, fill factor (FF), and PCE values of 0.75 V, 0.59, and 0.74%, respectively. The experimental data in this study revealed the fact that a PBDTThQx with acceptable photovoltaic properties would be a promising donor candidate for OPVs.

EXPERIMENTAL

Materials and Synthesis

All of the chemicals and reagents were obtained from Aldrich and Alfa Aesar and were used without further purification unless stated otherwise; 3,6-dibromo-1,2-phenylenediamine and 2,6-bis (trimethyltin)-4,8-bis(2-ethylhexyl)benzo[1,2-b:3,4-b′]dithiophene were synthesized according to the reported literature.[4]

1,2-Bis(5-octylthiophen-2-yl)ethane-1,2-dione (1). A mixture of 2-octylthiophene (5 g, 25.4 mmol) and dichloromethane (25 mL) was stirred at 0°C under a nitrogen atmosphere. $AlCl_3$ (3.38 g, 25.4 mmol) was added slowly to the suspension over a period of 30 min. Then, oxalyl chloride (1.47 g, 11.5 mmol) was added dropwise. The mixture was stirred for 3 h at 12°C. The solution was poured into ice–water with care and was extracted with dichloromethane. The organic layer was washed with brine and dried over anhydrous magnesium sulfate. After the removal of the solvent, the residue was recrystallized twice by hexane, and we obtained compound **1** (1.82 g, 4.05 mmol) in a 35.2% yield.

The ^{1}H-NMR spectrum of compound **1** is shown in Figure 1 (500 MHz, $CDCl_3$, ppm, δ): 7.86 (d, 2H, J = 3.5 Hz), 6.88

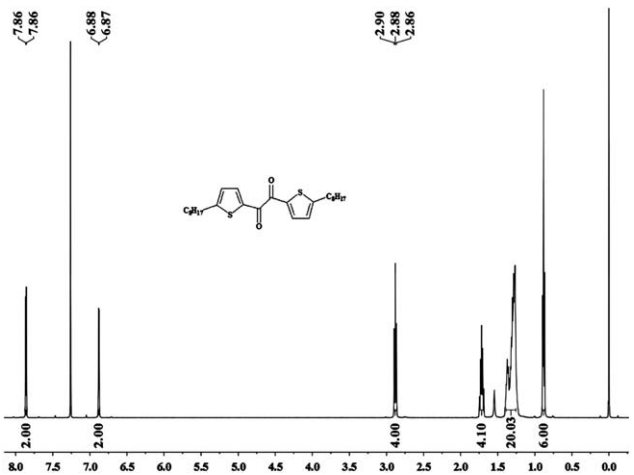

Figure 1. ^{1}H-NMR spectrum of compound **1** (at 500 MHz in $CDCl_3$).

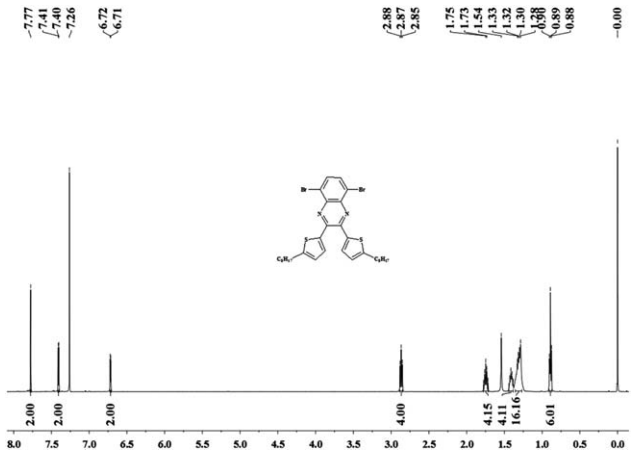

Figure 2. ^{1}H-NMR spectrum of compound Qx(Th) (at 500 MHz in $CDCl_3$).

(d, 2H, J = 5 Hz), 2.88 (t, 4H, J = 10 Hz), 1.72 (m, 4H), 1.37–1.26 (m, 20H), and 0.88 (t, 6H, J = 7 Hz).

5,8-Dibromo-2,3-bis(5-octylthiophen-2-yl) quinoxaline [Qx(Th)]. Compound **1** (2 g, 4.48 mmol) and 3,6-dibromo-1,2-phenylenediamine (1.43 g, 5.37 mmol) were dissolved in acetic acid (AcOH; 180 mL) and stirred at 40°C overnight. The precipitate was collected by filtration and washed with ethanol three times and purified by column chromatography with hexane–ethyl acetate (100:1), and we obtained Qx(Th) (2.35 g, 3.47 mmol) in a yield 77.5%.

The ^{1}H-NMR spectrum of Qx(Th) is provided in Figure 2 (500 MHz, $CDCl_3$, ppm): $\delta = 7.77$ (s, 2H), 7.41 (d, 2H, J = 5 Hz), 6.72 (d, 2H, J = 5 Hz), 2.87 (t, 4H, J = 5 Hz), 1.75 (m, 4H), 1.41 (m, 4H), 1.31 (m, 16H), 0.89 (t, 6H, J = 5 Hz).

PBDTThQx. In a 50-mL flask, Qx(Th) (203.6 mg, 0.3 mmol) and 2,6-bis(trimethyltin)−4,8-bis(2-ethylhexyl)benzo[1,2-b:3,4-b′]dithiophene (231.6 mg, 0.3 mmol) were dissolved in 20 mL of toluene and stirred at room temperature under a nitrogen atmosphere for 30 min. Then, tris(dibenzylideneacetone)dipalladium [$Pd_2(dba)_3$; 5.5 mg] and tris(*o*-tolyl)phosphine [$P(o\text{-}Tol)_3$; 7.3 mg] were added and flushed with nitrogen for another 30 min. After that, the reactants were stirred for 24 h at 110°C in the nitrogen atmosphere. After cooling, the solution was poured into methanol. The polymer was collected by filtration and Soxhlet-extracted with methanol, hexane, and chloroform in order. The chloroform solution was concentrated into a small volume and then poured into methanol again. The precipitate was collected by filtration and dried *in vacuo* at 50°C overnight, and this afforded PBDTThQx (252 mg) as a blue–black solid at a yield 87.5%.

Gel permeation chromatography (tetrahydrofuran, polystyrene standard, 25°C): number-average molecular weight = 84.8 kDa, weight-average molecular weight = 326.8 kDa, polydispersity index = 3.85.

ANAL. Calcd for $(C_{58}H_{76}N_2O_2S_4)_n$: C, 71.46%; H, 7.86%; *N*, 2.91%. Found: C, 72.45%; H, 7.97%; N, 2.91%.

Characterization

^{1}H-NMR spectra were recorded on a Bruker DRX-500 spectrometer (at 500 MHz). The molecular weights and distributions of the copolymer were determined by gel permeation chromatography. Tetrahydrofuran (THF) and polystyrene were used as the eluent and standard, respectively, during the measurement. The ultraviolet–visible (UV–vis) absorption spectra were recorded by a Unico UV-2102 scanning spectrophotometer. Thermogravimetric analyses (TGA) for the polymers was carried out on a Universal V2.4F (TA Instruments). The electrochemical cyclic voltammetry (CV) was carried out on a CHI 660D electrochemical workstation. A Pt disk, Pt plate, and Ag/Ag^+ electrode were used as the working electrode, counter electrode, and reference electrode, respectively, in a 0.1 mol/L tetrabutyl ammonium hexafluorophosphate (Bu_4NPF_6) acetonitrile solution. We produced polymer thin films by drop-casting 1.0 μL of PBDTThQx in THF solution (analytical reagent, 1 mg/mL) onto the working electrode (Pt disk) and then drying in air. The CV curves of the pristine PBDTThQx films were recorded by the electrochemical workstation. Additionally, the HOMO and lowest unoccupied molecular orbital (LUMO) energy levels of the PBDTThQx films were estimated by the CV measurement.

OPV Fabrication and Characterization

To investigate the photovoltaic characteristics of PBDTThQx, OPVs with the configuration of indium tin oxide (ITO)–poly(3,4-ethylenedioxythiophene) (PEDOT)–poly(styrene sulfonate) (PSS)–PBDTThQx–$PC_{61}BM$ (with weight ratios of 1:1, 1:2, 1:3, and 1:4)–LiF–Al were fabricated and characterized at room temperature under ambient conditions.

ITO (<20 Ω/□) evaporated on glass substrate was used as the anode. The ITO substrates were cleaned with deionized water, acetone, and anhydrous ethanol in sequence by an ultrasonic cleaner. Then, the ITO substrates were illuminated by UV and oxygen plasma for 5 min to remove organic contamination. PEDOT–PSS (Baytron P VPAl 4083) aqueous solution was spin-cast onto ITO substrates and then annealed at 200°C for 20 min under an N_2 atmosphere. A PEDOT–PSS layer with a

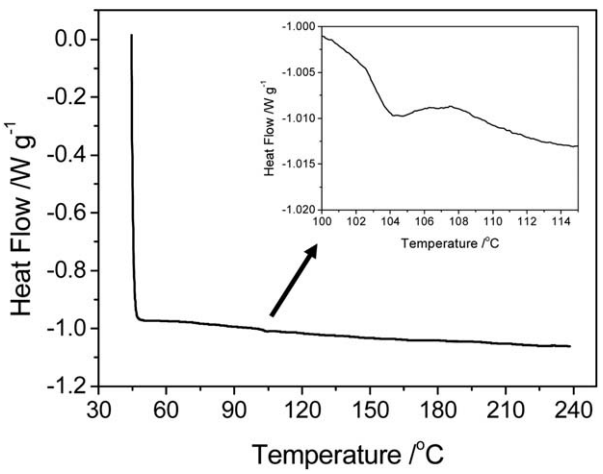

Figure 3. Differential scanning calorimetry measurements of PBDTThQx. The inset shows an enlarged plot of the glass-transition temperature point.

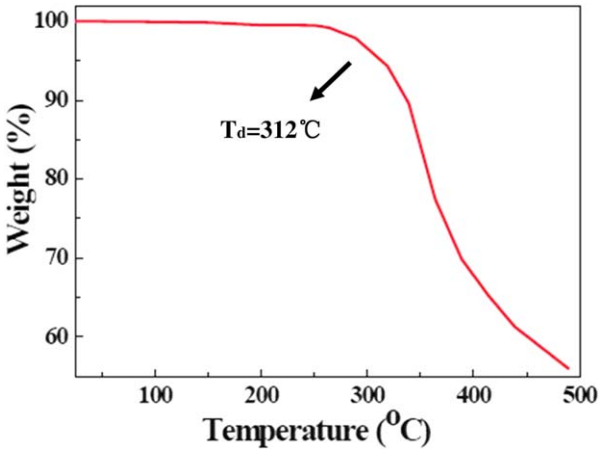

Figure 4. TGA curve of PBDTThQx. [Color figure can be viewed in the online issue, which is available at wileyonlinelibrary.com.]

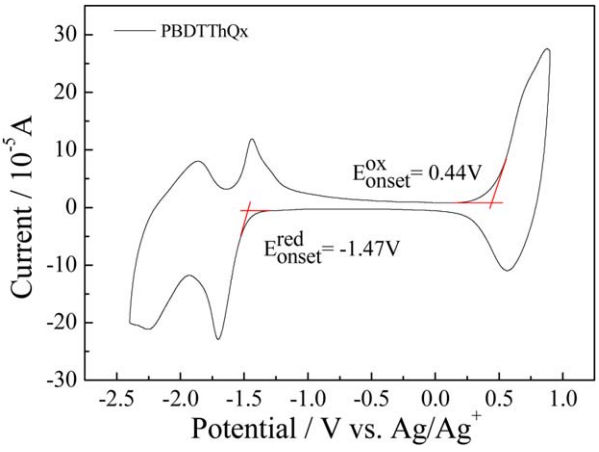

Figure 6. Cyclic voltammogram of the PBDTThQx films on a Pt electrode (0.1 mol/L Bu_4NPF_6 and CH_3CN solution at a scan rate of 100 mV/s). [Color figure can be viewed in the online issue, which is available at wileyonlinelibrary.com.]

thickness of about 28 nm performed as the anode buffer layer. PBDTThQx and $PC_{61}BM$ were simultaneously dissolved in chlorobenzene with a concentration of 10 mg/mL. For comparison, the weight ratios of PBDTThQx to $PC_{61}BM$ varied from 1:1 to 1:4. The PBDTThQx–$PC_{61}BM$ solutions were spin-coated onto the PEDOT–PSS layers. Then, the films were transferred immediately into a glovebox for solvent annealing at room temperature. The annealed PBDTThQx–$PC_{61}BM$ films were used as photoactive layers of the OPVs, and the thickness of the PBDTThQx–$PC_{61}BM$ films was gauged to be about 70 nm with atomic force microscopy (AFM) measurement. Finally, the cathode buffer layer (LiF) and cathode (Al) were thermally evaporated in sequence onto the active layers with evaporation rates of 0.1 and 2.5 Å/s, respectively. The LiF and Al layers were controlled to be 0.7 and 100 nm, respectively, by a quartz crystal microbalance in the vacuum chamber. The effective area of the OPVs was defined by a shadow mask with openings 2 mm in diameter.

The current density–voltage (*J–V*) data were measured with a Keithley 2611 source meter under illumination conditions (Newport Thermal Oriel 69911 300W, air mass (AM) 1.5G illumination at 100 mW/cm^2). A calibrated mono silicon diode was used as a reference. All of the OPVs were investigated without encapsulation.

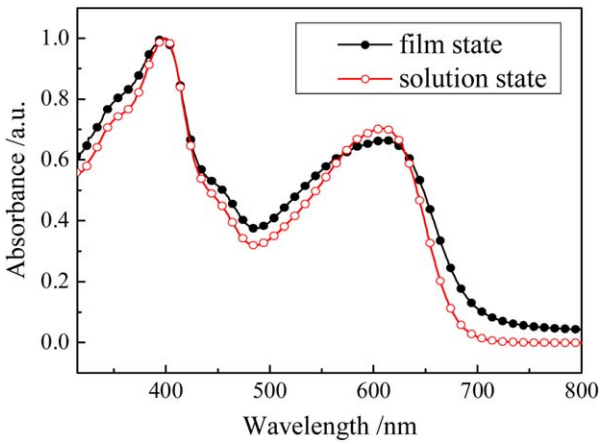

Figure 5. Absorption spectra of PBDTThQx in solution and film states. [Color figure can be viewed in the online issue, which is available at wileyonlinelibrary.com.]

RESULTS AND DISCUSSION

Thermal Properties

The thermal properties of PBDTThQx were analyzed by differential scanning calorimetry and TGA. The glass-transition temperature was observed around 104°C, as shown in Figure 3. Moreover, the decomposition temperature of PBDTThQx was located at 312°C (with 5% weight loss, as shown in Figure 4); this implied that PBDTThQx had good thermal stability for applications in OPVs.

Absorption Properties of PBDTThQx

The UV–vis absorption spectra of PBDTThQx were obtained both in the chloroform solution and in the film state, as shown in Figure 5. The absorption peaks of the PBDTThQx solution were almost identical to those in the film state. The peaks around 400 nm were attributed to the π–π^* transition of the conjugated backbone. Meanwhile, the peaks located at about 620 nm were ascribed to the charge transfer between the BDT

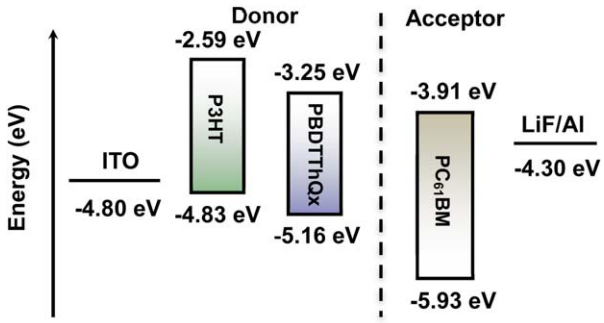

Figure 7. Schematic illustration of the energy levels of the materials used in the OPVs. [Color figure can be viewed in the online issue, which is available at wileyonlinelibrary.com.]

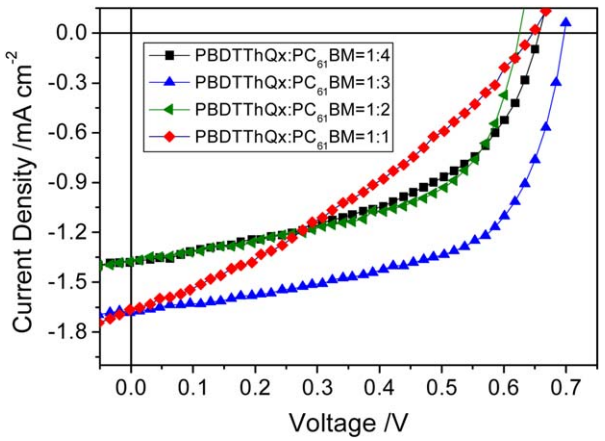

Figure 8. *J–V* characteristics of the photovoltaic device under an AM 1.5 G irradiation of 100 mW/cm^2. [Color figure can be viewed in the online issue, which is available at wileyonlinelibrary.com.]

and ThQx segments. Furthermore, the absorption edge of PBDTThQx in the film state was 705 nm, which was about 17 nm redshifted compared with that in the solution state. The bathochromic-shift phenomenon revealed that the π-stacked structure might have been formed in the PBDTThQx film state. The optical band gap (E_g^{opt}) of PBDTThQx was evaluated to be 1.76 eV (~0.02 eV smaller than that of PBDTQx[4]) according to the absorption edge value of the PBDTThQx film; this indicated

Table I. Photovoltaic Data for the Polymer Solar Cells

PBDTThQx/$PC_{61}BM$	V_{oc} (V)	J_{sc} (mA/cm^2)	FF	PCE (%)
1:1	0.79	1.69	0.33	0.44
1:2	0.72	1.38	0.55	0.54
1:3	0.75	1.68	0.59	0.74
1:4	0.66	1.38	0.48	0.44
P3HT/$PC_{61}BM$ (1:1)	0.59	7.48	0.67	2.94

that when the thiophene rings were introduced into the quinoxaline segments instead of the benzene rings, the prolonged conjugation length was obtained. A relatively low band gap of PBDTThQx facilitated a high absorption in green–red region of the solar spectrum. Thus, OPVs with acceptable photovoltaic behaviors were prospective.

Electrochemical Properties

The redox potentials of PBDTThQx were studied by CV measurement. The HOMO and LUMO values of PBDTThQx were calculated accordingly.[26–28] The energy level of ferrocene (Fc)/ferrocenium (Fc+) was −4.8 eV below the vacuum level.[29] The former potential of Fc/Fc+ was gauged to be 0.08 eV against Ag/Ag^+. As shown in Figure 6, the onset reduction potential (E_{onset}^{red}) and oxidation potential (E_{onset}^{ox}) of the PBDTThQx

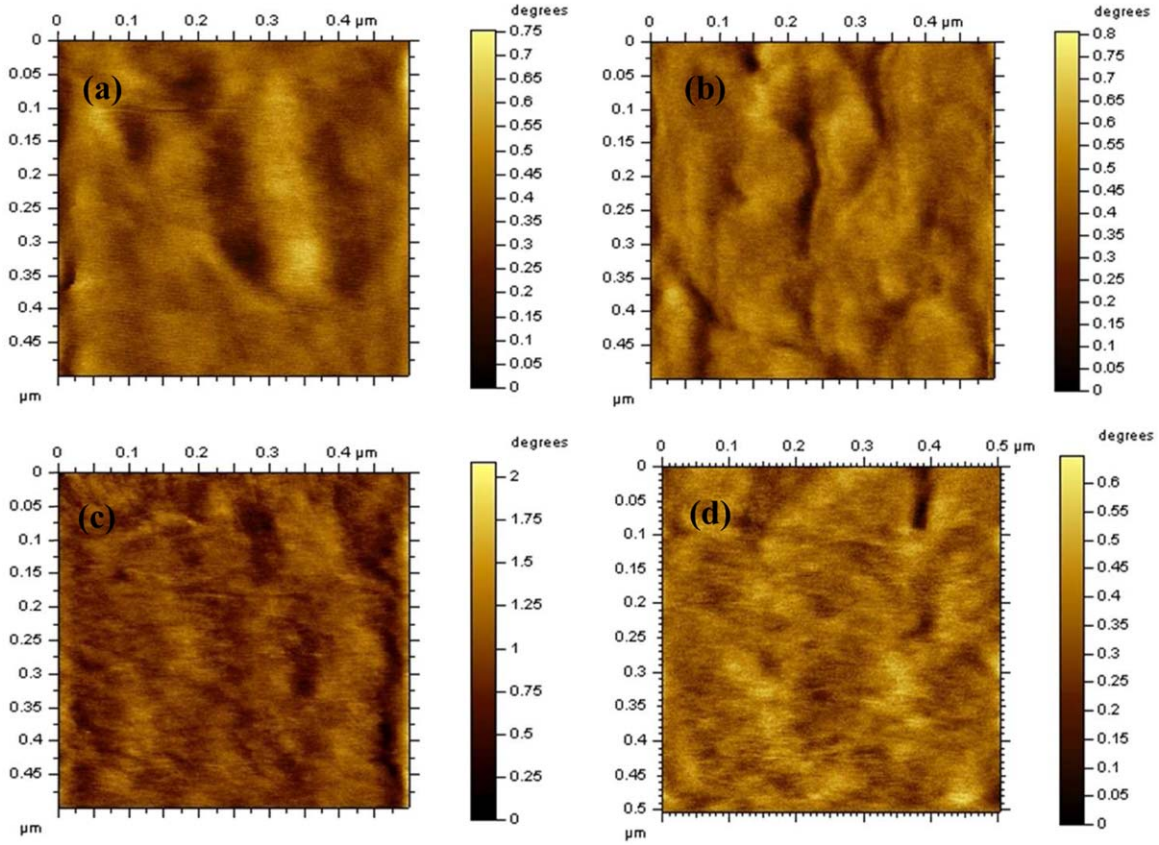

Figure 9. AFM phase images (0.5 × 0.5 μm^2) of PBDTThQx:$PC_{61}BM$ with weight ratios of (a) 1:1, (b) 1:2, (c) 1:3, and (d) 1:4. [Color figure can be viewed in the online issue, which is available at wileyonlinelibrary.com.]

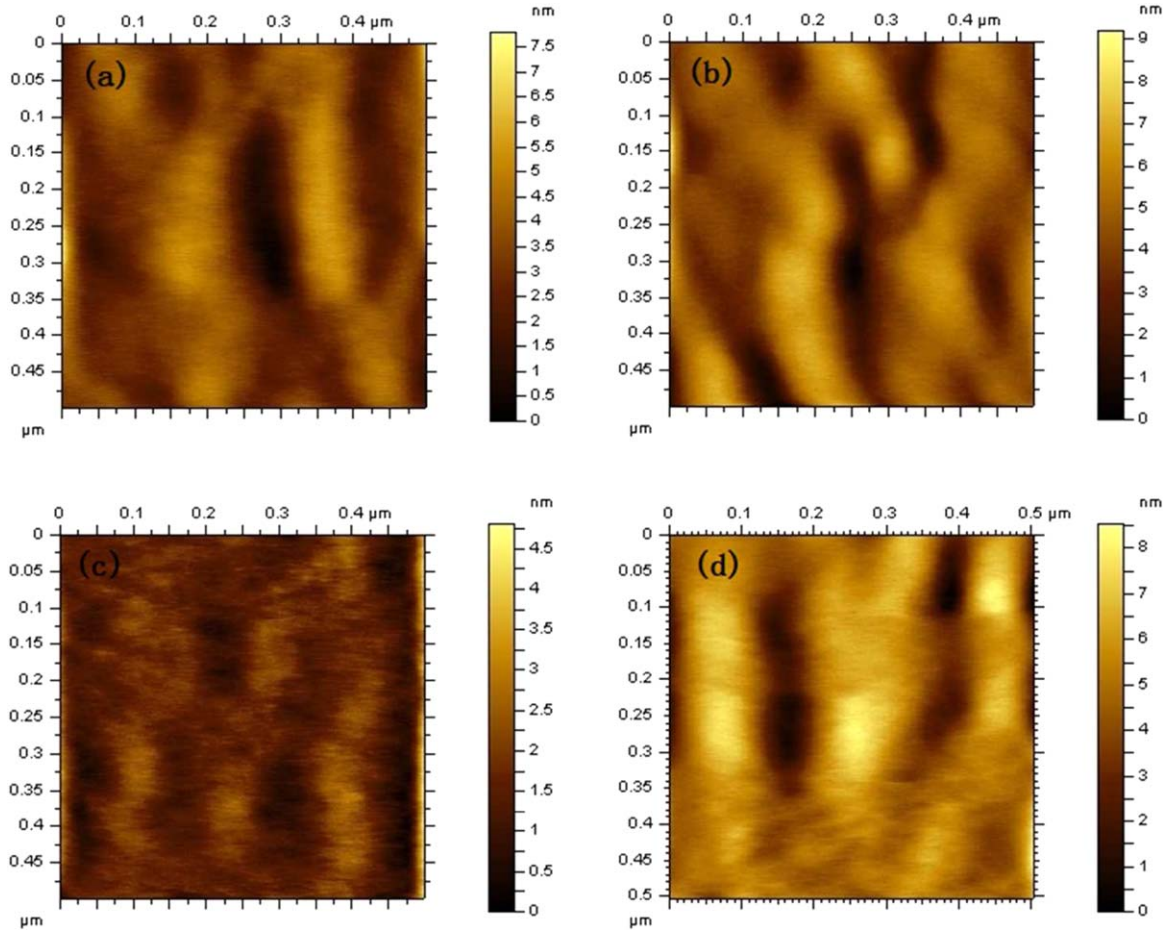

Figure 10. AFM topography images (0.5 × 0.5 μm^2) of PBDTThQx:$PC_{61}BM$ with weight ratios of (a) 1:1, (b) 1:2, (c) 1:3, and (d) 1:4. [Color figure can be viewed in the online issue, which is available at wileyonlinelibrary.com.]

film were recorded to be −1.47 and 0.44 V, respectively. Therefore, the HOMO and LUMO values of PBDTThQx were evaluated to be −5.16 and −3.25 eV, respectively. In addition, the electrochemical energy band gap of the PBDTThQx film was 1.91 eV, about 0.15 eV larger than the E_g^{opt} value. It was a common phenomenon that the electrochemical energy band gap value of the conjugated copolymers was higher than E_g^{opt}; this was mainly due to the energy barriers of the charge transfer at the electrodes during the CV measurement. The energy levels of the materials used in the OPVs are sketched in Figure 7. Levels of P3HT were also added for comparison. The HOMO level of PBDTThQx was about 0.33 eV lower than that of P3HT, as shown in Figure 7. This implied that the PBDTThQx-based OPVs might have possessed a higher V_{oc} than the P3HT-based counterparts. The LUMO level of PBDTThQx was 0.66 eV higher than that of $PC_{61}BM$; this induced electron-effective transfer at the donor–acceptor interface.

Photovoltaic Properties

To investigate the photovoltaic properties of PBDTThQx, the OPVs were fabricated with a typical configuration of ITO/PEDOT–PSS/PBDTThQx/$PC_{61}BM$/LiF/Al. PBDTThQx blended with the acceptor $PC_{61}BM$ performed as the active layer. The weight ratios of PBDTThQx to $PC_{61}BM$ varied from 1:1 to 1:4 for comparison. The *J–V* curves of the OPVs under the illumination of AM 1.5G (100 mW/cm^2) are recorded in Figure 8. The photovoltaic data are summarized in Table I. For comparison, a control device based on P3HT–$PC_{61}BM$ (1:1) was also fabricated in our laboratory, and the photovoltaic data are included in Table I. When the weight ratio of PBDTThQx to $PC_{61}BM$ reached 1:3, the corresponding OPV exhibited the best performance with V_{oc}, short-circuit current density (J_{sc}), FF, and PCE values of 0.75 V, 1.68 mA/cm^2, 0.59, and 0.74%, respectively. The improved photovoltaic properties of the OPV were attributed to the optimized phase separation of the PBDTThQx to $PC_{61}BM$ (1:3) active layer, and effective exciton diffusion and dissociation were realized accordingly.

The surface phase images of PBDTThQx to $PC_{61}BM$ with different blend ratios, as shown in Figure 9, were studied with tapping-mode AFM. When the weight ratio of PBDTThQx–$PC_{61}BM$ reached 1:3, a relatively finer domain size and a comparatively better phase separation were achieved, as shown in Figure 9(c). Moreover, to investigate the roughness of the PBDTThQx–$PC_{61}BM$ blend films, AFM topography images (0.5 × 0.5 μm^2) of the PBDTThQx–$PC_{61}BM$ films were also

obtained and are presented in Figure 10. The root mean square roughness of PBDTThQx–$PC_{61}BM$ (1:3) was gauged to be 0.504 nm; this was lower than that of any other blend film [1.02 nm for PBDTThQx–$PC_{61}BM$ (1:1), 1.32 nm for PBDTThQx–$PC_{61}BM$ (1:2), and 1.39 nm for PBDTThQx–$PC_{61}BM$ (1:4)], as shown in Figure 10. The flat surface of PBDTThQx–$PC_{61}BM$ (1:3) facilitated the fine contact between the active layer and cathode. Then, the effective electron extraction was realized. Therefore, the exciton dissociation and charge diffusion were optimized when the blend ratio of PBDTThQx–$PC_{61}BM$ was controlled to be 1:3,[30,31] and the photovoltaic performance was improved accordingly. However, much work is still required to effectively increase the J_{sc} value of the PBDTThQx-based OPVs. For example, we need to insert novel buffer layers into the device,[32,33] optimize the annealing treatment,[34,35] and modify the electrodes.[36,37] Therefore, PBDTThQx will be a promising donor candidate for photovoltaic devices, and further improvement in PBDTThQx-based OPVs can be foreseen.

CONCLUSIONS

A copolymer, PBDTThQx, based on BDT and ThQx moieties was synthesized and characterized with NMR, UV–vis spectroscopy, TGA, and CV. With a narrow band gap of 1.76 eV and a low HOMO of 5.16 eV, the PBDTThQx-based OPVs exhibited a broad absorption and high V_{oc}. When the weight ratio of PBDTThQx to $PC_{61}BM$ reached 1:3, satisfying photovoltaic properties were achieved. The experimental data revealed that PBDTThQx was a potential donor for OPVs, and the improved photovoltaic performance was promising.

ACKNOWLEDGMENTS

This work was supported by the National Basic Research Program through grant 2009CB930504 and the National Natural Science Foundation of China through grants 60907015, 60907012, 61177031, 61177020, 10934001, and 11121091. Bo Qu was also supported by the Research Fund for the Doctoral Program of Higher Education through grant 20110001120124.

REFERENCES

1. Chen, J. W.; Cao, Y. *Acc. Chem. Res.* **2009**, *42*, 1709.
2. Yu, G.; Gao, J.; Hummelen, J. C.; Wudi, F.; Heeger, A. *J. Science* **1995**, *270*, 1789.
3. Chen, G. Y.; Lan, S. C.; Lin, P. Y.; Chu, C. W.; Wei, K. H. *J. Polym. Sci. Part A: Polym. Chem.* **2010**, *48*, 4456.
4. Wu, H. M.; Qu, B.; Cong, Z. Y.; Liu, H. L.; Tian, D.; Gao, B. W.; An, Z. W.; Gao, C.; Xiao, L. X.; Chen, Z. J.; Liu, H. H.; Gong, Q. H.; Wei, W. *React. Funct. Polym.* **2012**, *72*, 897.
5. Lu, Y. Z.; Wang, Y.; Feng, Z. H.; Ning, Y.; Liu, X. J.; Lu, Y. W.; Hou, Y. B. *Synth. Met.* **2012**, *162*, 2039.
6. Ma, W. L.; Yang, C. Y.; Gong, X.; Lee, K.; Heeger, A. *J. Adv. Funct. Mater.* **2005**, *15*, 1617.
7. Zou, Y.; Najari, A.; Berrouard, P.; Beaupre, S.; Aich, B.-R.; Tao, Y.; Leclerc, M.; Thieno, A. *J. Am. Chem. Soc.* **2010**, *132*, 5330.
8. Takimiya, K.; Kunugi, Y.; Konda, Y.; Niihara, N.; Otsubo, T. *J. Am. Chem. Soc.* **2004**, *126*, 5084.
9. Kashiki, T.; Miyazaki, E.; Takimiya, K. *Chem. Lett.* **2009**, *38*, 568.
10. Chen, M.-C.; Kim, C.; Chen, S.-Y.; Chiang, Y.-J.; Chung, M.-C.; Facchetti, A.; Marks, T. J. *J. Mater. Chem.* **2008**, *18*, 1029.
11. Shinamura, S.; Osaka, I.; Miyazaki, E.; Nakao, A.; Yamagishi, M.; Takeya, J.; Takimiya, K. *J. Am. Chem. Soc.* **2011**, *133*, 5024.
12. Niimi, K.; Kang, M.-J.; Miyazaki, E.; Osaka, I.; Takimiya, K. *Org. Lett.* **2011**, *13*, 3430.
13. Loser, S.; Burns, C. J.; Miyauchi, H. R.; Ortiz, P.; Facchetti, A.; Stupp, S. I.; Marks, T. J. *J. Am. Chem. Soc.* **2011**, *133*, 8142.
14. Loser, S.; Miyauchi, H.; Hennek, J. W.; Smith, J.; Huang, C.; Facchetti, A.; Marks, T. *J. Chem. Commun.* **2012**, *48*, 8511.
15. Koti, R. S.; Sanjaykumar, S. R.; Hong, S. J.; Song, C. E.; Kang, I. N.; Lee, S. K.; Shin, W. S.; Moon, S. J.; Lee, J. C. *Sol. Energy Mater. Sol. Cells* **2013**, *108*, 213.
16. Wang, E.; Wang, L.; Lan, L.; Luo, C.; Zhuang, W.; Peng, J.; Cao, Y. *Appl. Phys. Lett.* **2008**, *92*, 033307.
17. Park, S. H.; Roy, A.; Beaupré, S.; Cho, S.; Coates, N.; Moon, J. S.; Moses, D.; Leclerc, M.; Lee, K.; Heeger, A. *J. Nat. Photonics* **2009**, *3*, 297.
18. Huo, L. J.; Guo, X.; Li, Y. F.; Hou, J. H. *Chem. Commun.* **2011**, *47*, 8850.
19. Zhang, Y.; Hau, S. K.; Yip, H. L.; Sun, Y.; Acton, O.; Jen, A. K.-Y. *Chem. Mater.* **2010**, *22*, 2696.
20. Price, S. C.; Stuart, A. C.; Yang, L.; Zhou, H.; You, W. *J. Am. Chem. Soc.* **2011**, *133*, 4625.
21. Huo, L. J.; Zhang, S. Q.; Guo, X.; Xu, F.; Li, Y. F.; Hou, J. H. *Angew. Chem. Int. Ed.* **2011**, *50*, 9697.
22. Carsten, B.; Szarko, J. M.; Lu, L. Y.; Son, H. J.; He, F.; Botros, Y. Y.; Chen, L. X.; Yu, L. P. *Macromolecules* **2012**, *45*, 6390.
23. Wang, E. G.; Hou, L. T.; Wang, Z. Q.; Hellström, S.; Zhang, F. L.; Inganäs, O.; Andersson, M. R. *Adv. Mater.* **2010**, *22*, 5240.
24. He, Z. C.; Zhang, C.; Xu, X. F.; Zhang, L. J.; Huang, L.; Chen, J. W.; Wu, H. B.; Cao, Y. *Adv. Mater.* **2011**, *23*, 3086.
25. Gao, Z.; Qu, B.; Wu, H.; Yang, H.; Gao, C.; Zhang, L.; Xiao, L.; Chen, Z.; Wei, W.; Gong, Q. *Synth. Met.* **2013**, *172*, 69.
26. Li, Y. F.; Cao, Y.; Gao, J.; Wang, D. L.; Yu, G.; Heeger, A. *J. Synth. Met.* **1999**, *99*, 243.
27. Sun, Q. J.; Wang, H. Q.; Yang, C. H.; Li, Y. F. *J. Mater. Chem.* **2003**, *13*, 800.
28. Hou, J. H.; Tan, Z. A.; Yan, Y.; He, Y. J.; Yang, C. H.; Li, Y. F. *J. Am. Chem. Soc.* **2006**, *128*, 4911.
29. Pommerehne, J.; Vestweber, H.; Guss, W.; Mahrt, R. F.; Bässler, H.; Porsch, M.; Daub, J. *Adv. Mater.* **1995**, *7*, 551.
30. Scully, S. R.; McGehee, M. D. *J. Appl. Phys.* **2006**, *100*, 034907.
31. Kim, B. J.; Miyamoto, Y.; Ma, B. W.; Fréchet, J. M. *J. Adv. Funct. Mater.* **2009**, *19*, 2273.

32. Chen, Y.; Jiang, Z. T.; Gao, M.; Watkins, S. E.; Lu, P.; Wang, H. Q.; Chen, X. W. *Appl. Phys. Lett.* **2012**, *100*, 203304.

33. Duan, C. H.; Zhong, C. M.; Liu, C. C.; Huang, F.; Cao, Y. *Chem. Mater.* **2012**, *24*, 1682.

34. Motaung, D. E.; Malgas, G. F.; Nkosi, S. S.; Mhlongo, G. H.; Mwakikunga, B. W.; Malwela, T.; Arendse, C. J.; Muller, T. F. G.; Cummings, F. R. *J. Mater. Sci.* **2013**, *48*, 1763.

35. Chambon, S.; Derue, L.; Lahaye, M.; Pavageau, B.; Hirsch, L.; Wantz, G. *Materials* **2012**, *5*, 2521.

36. Li, J. J.; Zuo, L. J.; Pan, H. B.; Jiang, H.; Liang, T.; Shi, Y.; Chen, H. Z.; Xu, M. S. *J. Mater. Chem. A* **2013**, *1*, 2379.

37. Yang, Q. Q.; Zhao, S. L.; Xu, Z.; Zhang, F. J.; Yan, G.; Kong, C.; Fan, X.; Zhang, Y. F.; Xu, X. R. *Chin. Phys. B* **2012**, *21*, 128402.